# Atomic layer deposition of two dimensional $MoS_2$ on 150 mm substrates

Arturo Valdivia
*School of EECS, Oregon State University, Corvallis, Oregon 97331*

Douglas J. Tweet
*Sharp Labs of America, Camas, Washington 98607*

John F. Conley, Jr.[a)]
*School of EECS, Oregon State University, Corvallis, Oregon 97331*

(Received 17 November 2015; accepted 21 January 2016; published 5 February 2016)

Low temperature atomic layer deposition (ALD) of monolayer to few layer $MoS_2$ uniformly across 150 mm diameter $SiO_2$/Si and quartz substrates is demonstrated. Purge separated cycles of $MoCl_5$ and $H_2S$ precursors are used at reactor temperatures of up to 475 °C. Raman scattering studies show clearly the in-plane ($E^1_{2g}$) and out-of-plane ($A_{1g}$) modes of $MoS_2$. The separation of the $E^1_{2g}$ and $A_{1g}$ peaks is a function of the number of ALD cycles, shifting closer together with fewer layers. X-ray photoelectron spectroscopy indicates that stoichiometry is improved by postdeposition annealing in a sulfur ambient. High resolution transmission electron microscopy confirms the atomic spacing of monolayer $MoS_2$ thin films. © *2016 American Vacuum Society*.
[http://dx.doi.org/10.1116/1.4941245]

## I. INTRODUCTION

The lack of a bandgap in graphene has led to the exploration of other 2D materials, in particular, transition metal dichalcogenides (TMDs). Like graphene, TMDs exist in a bulk state consisting of stacked planes held together through weak van der Waals forces. Each plane consists of a transition metal (M) from groups 4–10 and a group 16 chalcogen (X) to form a stoichiometric ratio of $MX_2$. Two dimensional TMDs that exhibit properties distinct from their bulk forms have recently come under intense investigation as building blocks for van der Waals heterostructure electronics.[1–5] One of the most promising TMDs is molybdenum disulfide ($MoS_2$).[6,7] The indirect bandgap (~1.2 eV) inherent to bulk $MoS_2$ transitions to a direct bandgap (~1.8 eV) in its monolayer state. The sizable direct bandgap makes $MoS_2$ a leading candidate material for low power digital electronics,[1,8] photonics,[1,9] sensing,[10] and catalysis applications.[11–13]

These potential applications require the preparation of high quality monolayer $MoS_2$ over large areas.[14,15] As with initial work on graphene, mechanically exfoliated $MoS_2$ has formed the base of much research into electronics applications.[5,8,10] However, the lack of scalability renders mechanical exfoliation impractical for manufacturing. Chemical vapor deposition (CVD) has been shown to yield $MoS_2$ on various substrates,[3,6] but exhibits drawbacks such as a lack of uniform electrical properties, poor process stability, and the high temperatures required (typically above 650 °C).[14–17]

A natural technique for the synthesis of 2D materials is atomic layer deposition (ALD). In ALD, film growth occurs via sequential, purge separated, self-limiting reactions of the precursors on the surface of the substrate. Sequential self-limiting surface reactions allow for precise thickness control, high conformality, and scalability to large surface areas, making ALD an ideal candidate for growing few layer TMDs.[18] Recently, ALD of monolayer $MoS_2$ thin films was reported for the first time using molybdenum (V) chloride ($MoCl_5$) and hydrogen disulphide ($H_2S$) precursors.[19] A shortcoming of this work was that single crystal ⟨0001⟩ orientation sapphire substrates (rather than Si) were required and depositions were limited to 2-in. diameter wafers. ALD of thick many layer $MoS_2$ films on $SiO_2$ and Si substrates was recently reported using molybdenum hexacarbonyl [$Mo(CO_6)$] and dimethyldisulfide [$CH_3$-S-S-$CH_3$] and $Mo(CO)_6$ and $H_2S$; however, monolayer growth was not achieved in either of these studies.[20,21]

In this work, we demonstrate that low temperature ALD can be used to deposit monolayer to few layer $MoS_2$ uniformly across 150 mm diameter $SiO_2$/Si and quartz substrates. $MoS_2$ material quality is assessed using Raman spectroscopy, photoluminescence, x-ray photoelectron spectroscopy, and transmission electron microscopy. The impact of postdeposition sulfur anneals on $MoS_2$ material quality is investigated.

## II. EXPERIMENT

ALD was conducted using a table top Arradiance Gemstar ALD system that was specially modified to handle $H_2S$ gas.[22] Substrate heating was performed using a platen holder to temperatures up to 475 °C at a base pressure of $3 \times 10^{-3}$ Torr. $MoCl_5$ and $H_2S$ precursors were alternately pulsed into the chamber using 20 sccm of $N_2$ as a carrier gas. The solid precursor $MoCl_5$ was heated to a temperature of 70 °C. The ALD pulse sequence included an additional "soak" step after each precursor pulse to ensure adequate time for reaction between the reactant ($MoCl_5$ or $H_2S$) and the respective surface species.[23] In all depositions, the $MoCl_5$ was pulsed first. The pulsing sequence used consisted of: 500 ms pulse $MoCl_5$/5 s soak/10 s $N_2$ purge/40 ms pulse $H_2S$/5 s soak/10 s $N_2$ purge. ALD $MoS_2$ thin films were deposited on 150 mm diameter (1) n-type Si wafers with

a)Electronic mail: jconley@eecs.oregonstate.edu

280 nm of thermally grown $SiO_2$ and (2) quartz wafers. Prior to ALD, the $SiO_2$/Si substrates were patterned with photoresist, and the oxide was etched via reactive ion etching to a depth of 40 nm, as shown in Fig. 1. After the etch process, the photoresist was ashed and the surface of the wafers was cleaned with piranha solution (sulfuric acid and hydrogen peroxide) followed by a 20–30 s short dip in dilute hydrofluoric acid. The $SiO_2$ mesas were created to promote the nucleation of $MoS_2$.[16] Following deposition, some as-deposited films were annealed in a sulfur environment by either (1) flowing 50 sccm $H_2S$ or (2) flowing Ar carrier gas over elemental sulfur heated to roughly 120–130 °C. All anneals were performed in a tube furnace for 30 min between 600 and 900 °C.

Raman analysis and photoluminescence (PL) was conducted using a WiTec Confocal Raman Microscope Alpha300 RA system with a 532 nm excitation laser. X-ray photoelectron spectroscopy (XPS) was conducted on a Thermo Scientific ESCALAB 250. Transmission electron microscopy (TEM) was performed on a FEI TITAN 80–200 TEM/SEM with ChemiSTEM technology.

## III. RESULTS AND DISCUSSION

Shown in Fig. 2 are photographs of two 150 mm quartz wafers placed on a chemwipe (a) pre- and (b) post-ALD. Following 50 ALD cycles of $MoCl_5$ and $H_2S$ at 475 °C, the quartz wafer in Fig. 2(b) changes to a dark yellow (color online) shade that is visually uniform across the full wafer.

Shown in Fig. 3(a) are Raman spectra comparing the etched and unetched regions of a patterned $SiO_2$/Si wafer following 50 cycles of ALD at 375 °C. The characteristic in-plane ($E^1_{2g}$) and out-of-plane ($A_{1g}$) vibrational modes of $MoS_2$ appear in both Raman spectra near 382 and 404 $cm^{-1}$, respectively, indicating an ordered S-Mo-S atomic arrangement.[24,25] The dashed lines at 383 and 408 $cm^{-1}$ indicate the position of these two peaks measured in a bulk $MoS_2$ sample. The $E^1_{2g}$ and $A_{1g}$ peaks in the unetched region are more distinct and of a higher intensity compared to those observed in the etched region, indicating preferential growth of $MoS_2$ in the unetched region. Deposition of $MoS_2$ was also attempted on a blanket $SiO_2$/Si wafer with no patterning. Raman analysis of the blanket $SiO_2$/Si substrate showed the absence of both the $E^1_{2g}$ and $A_{1g}$ peaks, suggesting that the enhanced growth on unetched regions of $SiO_2$ may be due to residual photoresist acting as additional nucleation sites.[16]

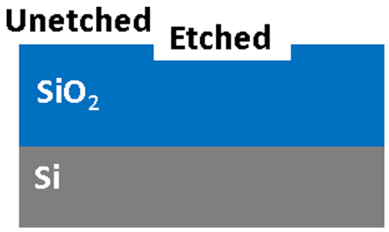


FIG. 1. (Color online) Schematic cross section of patterned $SiO_2$/Si substrate.

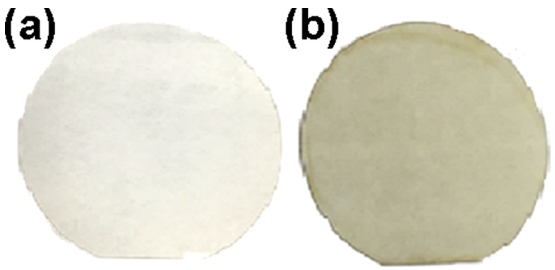


FIG. 2. (Color online) Photographs of 150 mm quartz wafers: (a) uncoated and (b) after 50 cycles of ALD $MoS_2$ at 475 °C.

Shown in Fig. 3(b) are plots of Raman intensity versus wave number for 50 cycle ALD $MoS_2$ as-deposited at either 375 or 475 °C on the unetched region of a patterned $SiO_2$/Si wafer. The $E^1_{2g}$ and $A_{1g}$ peaks are significantly sharper and of higher intensity at the 475 °C deposition temperature, indicating higher quality growth.

The properties of the as-deposited ALD $MoS_2$ films are improved by annealing in a sulfur ambient. Shown in Fig. 4(a) are plots of Raman intensity versus wave number for as-deposited and sulfur annealed $MoS_2$ films from the unetched region of a patterned $SiO_2$/Si wafer. All data were normalized to the Si peak at 520 $cm^{-1}$ (not shown). For

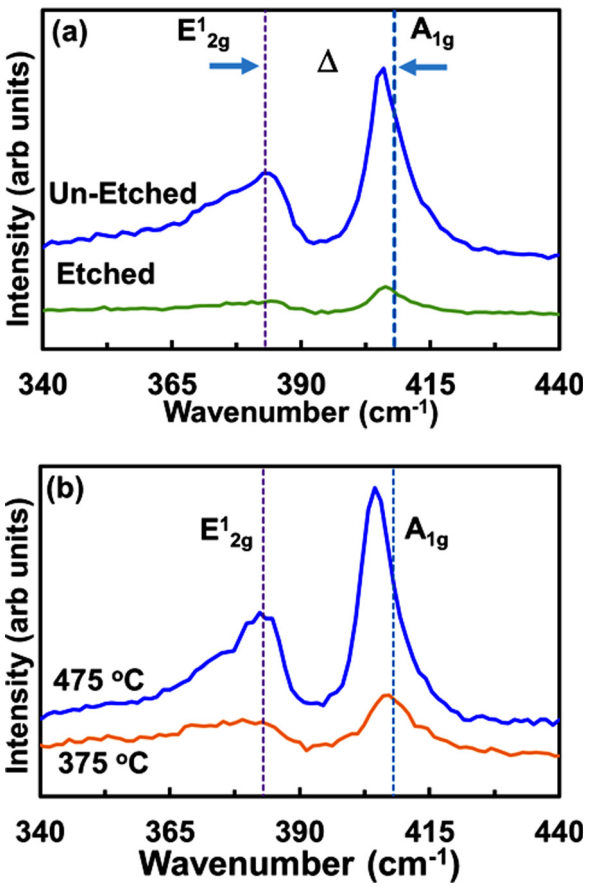


FIG. 3. (Color online) (a) Raman spectra of 375 °C as-deposited ALD $MoS_2$ films on etched and unetched regions of a patterned $SiO_2$/Si wafer. (b) Raman spectra comparing ALD $MoS_2$ as-deposited at either 375 or 475 °C on the unetched region of a patterned $SiO_2$/Si wafer. The vertical dashed lines indicate the position of the $E^1_{2g}$ and $A_{1g}$ peaks for bulk $MoS_2$.

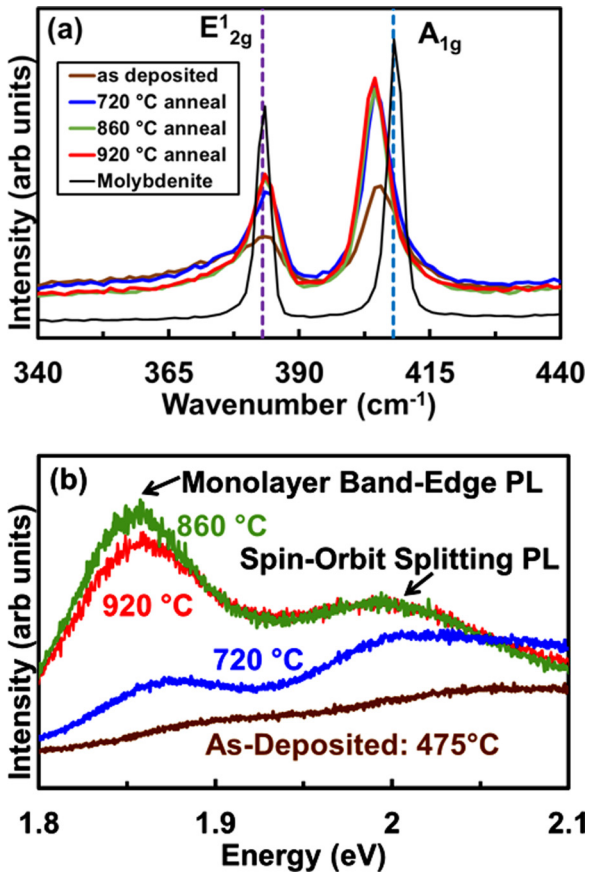


FIG. 4. (Color online) Raman spectra of 475 °C as-deposited and sulfur annealed ALD $MoS_2$ films showing (a) the region of the $E^1_{2g}$ and $A_{1g}$ peaks (a molybdenite spectrum is shown for reference) and (b) the region of the band-edge monolayer photoluminescence and spin-orbit splitting peaks.

reference, a Raman spectrum of bulk molybdenite is also shown. The full width half max (FWHM) of the $E^1_{2g}$ and $A_{1g}$ peaks are an indication of crystalline quality. After the sulfur anneal, the two characteristic $MoS_2$ peaks become narrower, stronger, and more symmetric. The FWHM of the $E^1_{2g}$ peak for the as-deposited ALD films is 18.3 $cm^{-1}$. The FWHM is reduced to 11.8 $cm^{-1}$ after annealing in sulfur ambient at 720 °C and further reduced to 4.2 $cm^{-1}$, comparable to CVD $MoS_2$,[15] after annealing at 920 °C. This suggests improved crystallinity with high temperature sulfur anneals. Even after the sulfur anneals, the FWHM of the $E^1_{2g}$ peak is still broader than 3.7 $cm^{-1}$, the FWHM of $MoS_2$ monolayers mechanically exfoliated from bulk $MoS_2$.[15]

Plots of PL versus energy in Fig. 4(b) show that in addition to the sharpening of the $E^1_{2g}$ and $A_{1g}$ peaks, the sulfur anneals result in the appearance of a strong PL peak at 1.86 eV, consistent with band edge emission from the direct bandgap of monolayer $MoS_2$.[11,26] The broad peak near 2.0 eV has been attributed to spin-orbit splitting from the band edge and is also associated with monolayer semiconducting $MoS_2$.[27,28] The PL peak is below the detection limit in the as-deposited films, begins to appear at 720 °C, strengthens at 860 °C, and decreases somewhat at 920 °C. Similar results are seen for $H_2S$ anneals.

XPS spectra for as-deposited 475 °C ALD $MoS_2$ films, along with films annealed in $H_2S$ at 600, 860, and 900 °C are shown in Fig. 5. The $Mo3d_{5/2}$ peaks and the $S2p_{3/2}$ peaks are resolved in Figs. 5(a) and 5(b), respectively, and correlate well to what has been previously reported in literature for $MoS_2$.[6] The ratio of the $S2p_{3/2}$ and $Mo3d_{5/2}$ peaks may be used to determine the stoichiometric ratio of the as-deposited and annealed films. The as-deposited films showed a S/Mo ratio of 1.4, indicating sulfur deficiency. This is consistent with the presence of the 236 eV peak in these films, which has been attributed to the $Mo^{6+}$ state.[28] After $H_2S$ annealing at 600 °C and above, the S/Mo ratio increased to the desired value of 2.0 and the 236 eV peak almost completely disappears, indicating that the $H_2S$ anneal is effective in improving stoichiometry as well as reducing defects.

Assessing the thickness of a 2D film is challenging. It has been shown that the number of $MoS_2$ layers present in a thin film may be determined by the frequency and separation ($\Delta$) between the $E^1_{2g}$ and $A_{1g}$ peaks.[24,25] It was reported that $\Delta$ increases with the number of S-Mo-S layers, with a monolayer having $\Delta \sim 19\ cm^{-1}$ and bulk like (>5 layers) $MoS_2$ having $\Delta \sim 25\ cm^{-1}$.[24,25] Shown in Fig. 6 is a plot of average $\Delta$ versus the number of ALD cycles for as-deposited 375 °C films. Qualitatively, $\Delta$ increases with the number of ALD cycles. Also shown are 50 cycle 475 °C films both as-deposited and annealed at 920 °C. The $\Delta$'s for the 25 and 50 cycle 375 °C as well as for the 50 cycle 475 °C as-deposited films are in the range of 22–23 $cm^{-1}$, correlating roughly to bilayer growth in the previous reports.[24,25] It should be noted

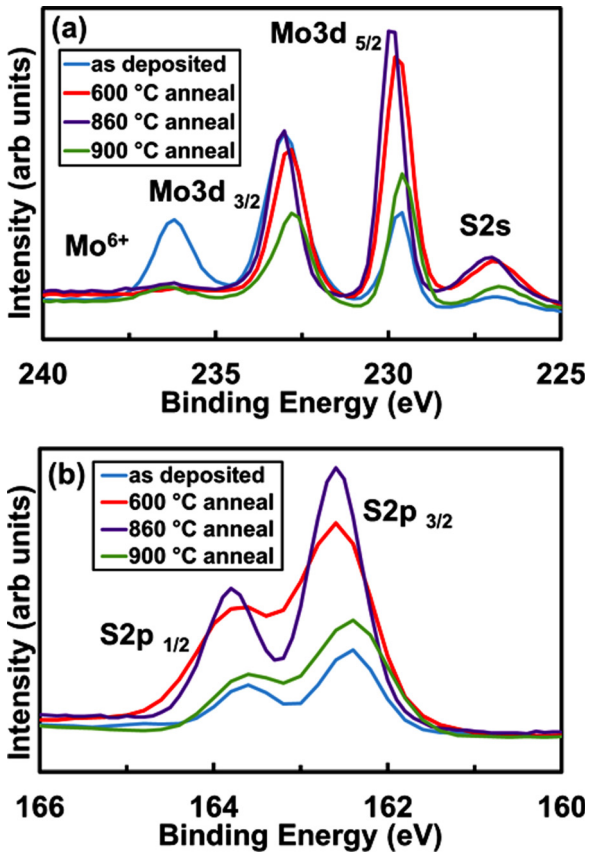


FIG. 5. (Color online) XPS spectra of (a) $Mo3d_{3/2}$ and (b) $S2p_{1/2}$ peaks for ALD $MoS_2$ films as-deposited at 475 °C and $H_2S$ annealed at either 600, 860, or 900 °C.

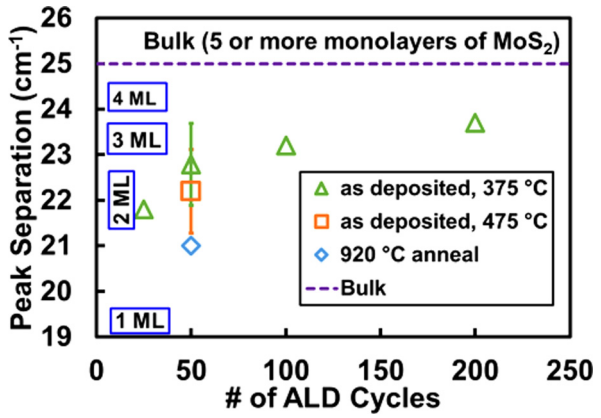


FIG. 6. (Color online) $E^1_{2g}$-$A_{1g}$ average peak separation (Δ) versus number of ALD cycles for 375 °C ALD $MoS_2$ films as-deposited on the unetched regions. Also shown are 475 °C films, as-deposited and annealed in sulfur at 920 °C.

however, that the position of the $A_{1g}$ peak may be sensitive to defects and substoichiometry. As indicated by the XPS results in Fig. 5, the as-deposited films are substoichiometric. Thus, the correlation here between Δ and the number of monolayers for the as-deposited films should be considered tentative. The Δ after annealing at 920 °C in sulfur decreases to about 21 $cm^{-1}$, suggestive of a mix of 1 and 2 monolayers.[24,25] This reduced Δ could be due either to an actual reduction of film thickness or improvement of stoichiometry (XPS results in Fig. 5 indicate that stoichiometry is improved by annealing). In either case, the accompanying appearance of clearly visible PL and spin orbit splitting peaks in Fig. 4(b) strongly suggests a mix of 1 and 2 monolayer regions.

Cross-sectional TEM images are shown in Fig. 7 for 50 cycle 375 °C ALD $MoS_2$ on the unetched region of the patterned $SiO_2$/Si substrate. The high resolution TEM in Fig. 7(b) verifies the existence of 1–2 monolayers of $MoS_2$. The intensity profile in Fig. 7(c) indicates the atomic lattice spacing to be to be approximately 0.29 nm for the (100) planes, consistent with the 0.31 nm atomic spacing of exfoliated hexagonal $MoS_2$.[29]

Finally, to confirm that the $MoS_2$ crystals are lying flat with their basal planes parallel to the substrate surface, rather than at a random or some other orientation, a polarization test was performed with the Raman instrument. The $E^1_{2g}$ peak is due to vibrational modes in the basal plane, while $A_{1g}$ peak is due to perpendicular modes.[24] By polarizing the incident laser beam and rotating the analyzer polarization, the $A_{1g}$ peak should be eliminated if the $MoS_2$ crystals are indeed lying flat on the substrate. Figure 8 shows Raman measurements taken with the analyzer in two positions 90° apart on a 50 ALD cycle sample deposited at 475 °C and annealed at 860 °C in sulfur. The $A_{1g}$ peak is almost entirely suppressed while the $E^1_{2g}$ peak is unaffected, confirming that the $MoS_2$ crystals have the desired orientation parallel to the surface.

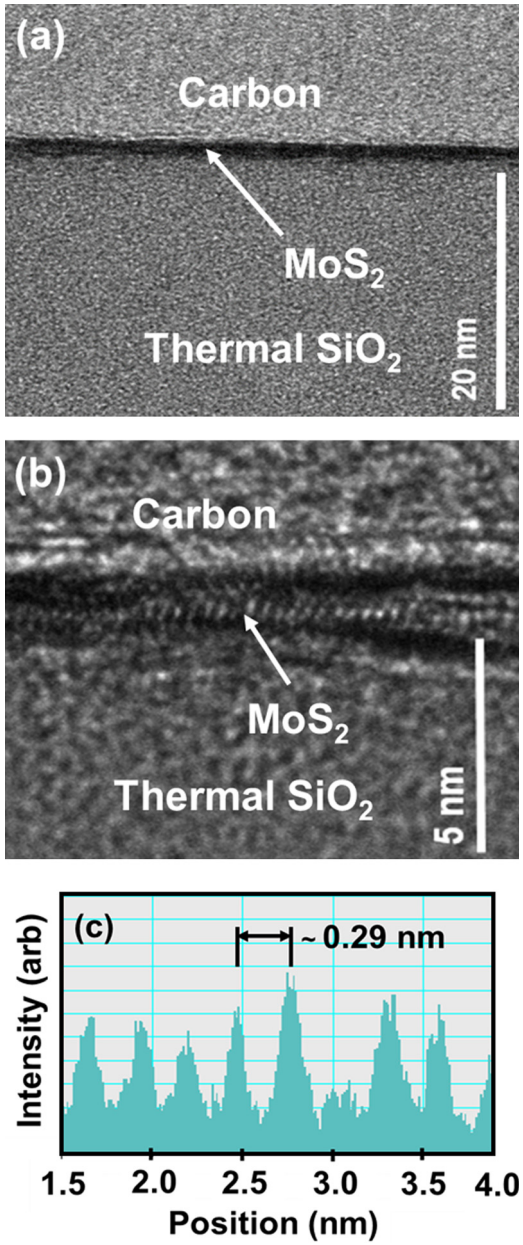


FIG. 7. (Color online) (a) TEM cross section of 50 cycle 375 °C ALD $MoS_2$ film as-deposited on unetched $SiO_2$/Si, (b) high resolution TEM image, and (c) intensity profile showing the atomic spacing.

## IV. SUMMARY AND CONCLUSIONS

In summary, ALD of monolayer to a few layered $MoS_2$ thin films was achieved uniformly across 150 mm quartz and patterned $SiO_2$/Si wafers using alternating pulses of $MoCl_5$ and $H_2S$. $MoS_2$ deposition was favored in unetched $SiO_2$ regions of patterned $SiO_2$/Si wafers. The as-deposited films show the characteristic Raman modes ($E^1_{2g}$ and $A_{1g}$) and $E^1_{2g}$-$A_{1g}$ separation associated with monolayer to few layer $MoS_2$. Raman polarization tests confirm the $MoS_2$ crystals have the desired orientation parallel to the surface. High temperature $H_2S$ and sulfur annealed films produce a sharpening of the $E^1_{2g}$ and $A_{1g}$ peaks as well as the appearance of the band edge PL and spin orbit splitting peaks, further indication of the presence of monolayer $MoS_2$. Hi-resolution TEM images confirm the presence of monolayer to bilayer $MoS_2$ films. XPS measurements indicate that a substoichiometric sulfur ratio in the as-deposited films is increased to the stoichiometric S/Mo ratio after annealing in $H_2S$ at

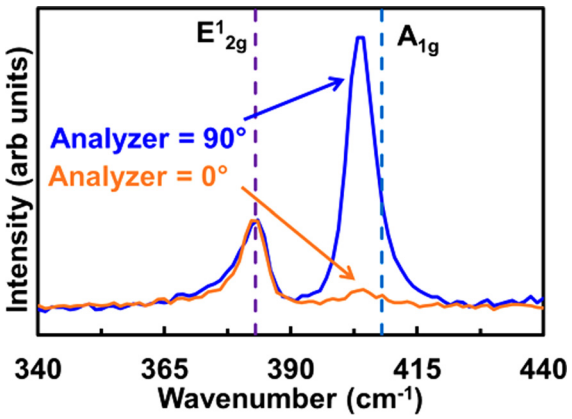


FIG. 8. (Color online) Raman spectra taken with the analyzer polarizer rotated at 90° and at 0°. Both in-surface ($E^1_{2g}$) and normal-to-surface ($A_{1g}$) oscillations come through at 90° but at 0° the Raman light scattered from modes normal-to-surface ($A_{1g}$) are blocked, suggesting the $MoS_2$ crystals have their c-axis normal to surface.

600 °C and above. Overall ALD is shown to be a promising method for uniform deposition of monolayer $MoS_2$ over large surface areas. The small crystallite sizes obtained may be suitable for application to hydrogen evolution catalysis.[4]

## ACKNOWLEDGMENTS

This work was supported by Sharp Labs of America (SLA) with matching funds from the Oregon Nanoscience and Microtechnologies Institute (ONAMI) and Oregon BEST. XPS was conducted by Fallon Fumasi at the Center for Advanced Materials Characterization in Oregon (CAMCOR) at the University of Oregon. TEM was conducted with the assistance of Pete Eschbach at the OSU Electron Microscopy Facility which is supported by the National Science Foundation via the Major Research Instrumentation (MRI) Program under Grant No. 1040588.

[1]Q. H. Wang, K. Kalantar-Zadeh, A. Kis, J. N. Coleman, and M. S. Strano, Nat. Nanotechnol. **7**, 699 (2012).
[2]A. K. Geim and I. V. Grigorieva, Nature **499**, 419 (2013).
[3]M. Chhowalla, H. S. Shin, G. Eda, L. Li, K. P. Loh, and H. Zhang, Nat. Chem. **5**, 263 (2013).
[4]A. Y. S. Eng, A. Ambrosi, Z. Sofer, P. Simek, and M. Pumera, ACS Nano **8**, 12185 (2014).
[5]Y. Lin *et al.*, ACS Nano **8**, 3715 (2014).
[6]X. Huang, Z. Zeng, and H. Zhang, Chem. Soc. Rev. **42**, 1934 (2013).
[7]W. Zhu, T. Low, Y. Lee, H. Wang, D. B. Farmer, J. Kong, F. Xia, and P. Avouris, Nat. Commun. **5**, 3087 (2014).
[8]B. Radisavljevic, A. Radenovic, J. Brivio, V. Giacometti, and A. Kis, Nat. Nanotechnol. **6**, 147 (2011).
[9]M. Tsai, S. Su, J. Chang, D. Tsai, C. Chen, C. Wu, L. Li, L. Chen, and J. He, ACS Nano **8**, 8317 (2014).
[10]H. Li *et al.*, Small **8**, 63 (2012).
[11]G. Eda, H. Yamaguchi, D. Voiry, T. Fujita, M. Chen, and M. Chhowalla, Nano Lett. **11**, 5111 (2011).
[12]Y. Li, H. Wang, W. L. Xie, Y. Liang, G. Hong, and H. Dai, J. Am. Chem. Soc. **133**, 7296 (2011).
[13]S. Shin, Z. Jin, D. H. Kwon, R. Bose, and Y. Min, Langmuir **31**, 1196 (2015).
[14]K. Kang, S. Xie, L. Huang, Y. Han, P. Y. Huang, K. F. Mak, C. Kim, D. Muller, and J. Park, Nature **520**, 656 (2015).
[15]Y. Yu, C. Li, Y. Liu, L. Su, Y. Zhang, and L. Cao, Sci. Rep. **3**, 1866 (2013).
[16]S. Najmaei *et al.*, Nat. Mater. **12**, 754 (2013).
[17]X. Ling, Y. Lee, Y. Lin, W. Fang, L. Yu, M. S. Dresselhaus, and J. Kong, Nano Lett. **14**, 464 (2014).
[18]V. Miikkulainen, M. Leskela, M. Ritala, and R. L. Puurunen, J. Appl. Phys. **113**, 021301 (2013).
[19]L. K. Tan, B. Liu, J. H. Teng, S. Guo, H. Y. Low, and K. P. Loh, Nanoscale **6**, 10584 (2014).
[20]Z. Jin, S. Shin, D. H. Kwon, S. Han, and Y. Min, Nanoscale **6**, 14453 (2014).
[21]D. K. Nandi, U. K. Sen, D. Choudhury, S. Mitra, and S. K. Sarkar, Electrochim. Acta **146**, 706 (2014).
[22]N. P. Dasgupta, J. F. Mack, M. C. Langston, A. Bousetta, and F. B. Prinz, Rev. Sci. Instrum. **81**, 044102 (2010).
[23]S. W. Smith, C. Beusch, D. J. Matthews, J. Simonsen, and J. F. Conley, Jr., J. Vac. Sci. Technol., A **32**, 041508 (2014).
[24]C. Lee, H. Yan, L. E. Brus, T. F. Heinz, J. Hone, and S. Ryu, ACS Nano **4**, 2695 (2010).
[25]H. Li, Q. Zhang, C. C. R. Yap, B. K. Tay, T. H. T. Edwin, A. Olivier, and D. Baillargeat, Adv. Funct. Mater. **22**, 1385 (2012).
[26]K. F. Mak, C. Lee, J. Hone, J. Shan, and T. F. Heinz, Phys. Rev. Lett. **105**, 136805 (2010).
[27]A. Splendiani, L. Sun, Y. B. Zhang, T. S. Li, J. Kim, C. Y. Chim, G. Galli, and F. Wang, Nano Lett. **10**, 1271 (2010).
[28]N. Kang, H. P. Paudel, M. N. Leuenberger, L. Tetard, and S. I. Khondaker, J. Phys. Chem. C **118**(36), 21258 (2014).
[29]H. E. Swanson, N. T. Gilfrich, and G. M. Ugrinic, "Standard x-ray diffraction powder patterns," in NBS Circular No. 539 (1955), Vol. 5, available at http://babel.hathitrust.org/cgi/pt?id=mdp.39015011413997;view=1up;seq=51.